PHASE EQUILIBRIUM STUDIES ON TiO_2-RICH SLAGS

Hanlie du Plooy and P.Chris Pistorius
Department of Materials Science and Metallurgical Engineering
University of Pretoria
0002 PRETORIA
Republic of South Africa
(+2712)4202187

Previously published results on phase relationships in the FeO-TiO_2 binary system are not consistent and not clearly defined for slags containing 80%TiO_2 or higher. These phase relations are of particular importance since a TiO_2 content of higher than 85% and a FeO content of approximately 10% are typical in modern ilmenite smelting operations. A technique for the rapid determination of the liquid-solid phase transition temperatures of such oxide systems containing more than 85%TiO_2 (with melting points typically higher than 1600 °C [2900 °F]), has been developed. The technique is based on the recording of cooling curves for a specimen which is heated in a thermocouple which doubles as a heating element. Undercooling or related effects are invariably present at the resulting high cooling rate, and procedures have been developed to avoid the effects of undercooling on the measurement of phase transformation temperatures.

1. INTRODUCTION

A TiO_2 content in the slag of 85% and higher is required in modern ilmenite processing. FeO (serving to fluidise the slag) is the other major slag component; hence an industrial slag may be approximated by the binary FeO-TiO_2 system. Although the binary FeO-TiO_2 phase diagram has been reported, the data are neither consistent, nor well defined for TiO_2 contents of 80% and higher[1,2,3].

The liquidus temperatures in the TiO_2-rich region are above 1650 °C (3000 °F), and thus difficult to measure. One possible approach is to apply high temperature microscopy, using visual inspection to detect the presence of crystals or liquid in the slag sample[4,5]. However, in this work it was found that slags containing FeO are opaque, ruling out this approach. Instead, thermal analysis was applied: the effect of the heat of solidification on the cooling curves was used to detect phase transformations.

2. EXPERIMENTAL TECHNIQUE

2.1 Thermocouple configuration

A thermocouple was employed as both sample holder and heating element, figure 1. To serve as sample holder, the two legs of the thermocouple (wire diameter 0.45 mm [0.0177"]), were bent parallel at the hot junction, leaving a space of 0.25 mm (0.0098") between the two wires. The thermocouple tip – approximately 7 to 10 mm (0.28 to 0.39") long – consisted of single wires, whereas the remaing lengths of the legs were constructed of two wires of the same composition twisted together (this was done to ensure that the hottest point during heating is at the thermocouple tip, by using the twin wires as heat sinks). These twin wires passed through a double bore ceramic tube with a length of 5 mm (0.20"), beyond which they were connected to water-cooled brass tubes which conducted the heating current. For measurement of the thermal EMF, compensation wire was connected to the cooled ends of the thermocouple wires. Both a type B thermocouple (Pt-6%Rh/Pt-30%Rh) and the nonstandard Pt-20%Rh/Pt-40%Rh thermocouple were used. The latter thermocouple can be used at temperatures up to 1880 °C (3416 °F), while the maximum temperature of the former is limited to approximately 1750 °C (3200 °F).

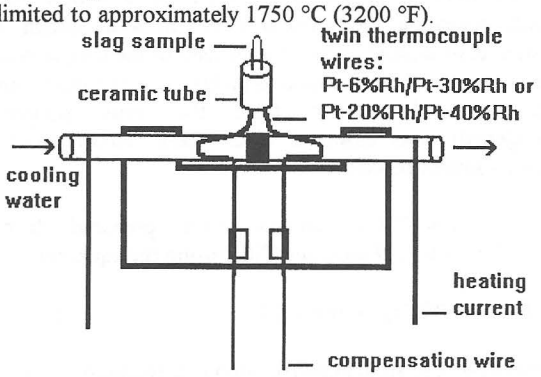

Fig. 1. The thermocouple configuration for thermal analysis.

The heating current which passed through the thermocouple was under thyristor control. The resulting potential variation across the thermocouple followed an altered sine wave, as illustrated in figure 2.

The thermocouple tip was inserted into a gas tight cell with the tip pointing downwards. Slag samples were placed into the thermocouple tip at the hot junction. The sample was kept in place by gravity and capillary forces. The mass of each slag sample was approximately 4 mg ($9x10^{-6}$ lb). A dried and deoxidised argon atmosphere was maintained in the cell during heating and cooling.

2.2 Sample preparation

Two compositions from the CaO-SiO_2-system (with known liquidus and solidus temperatures) were used to test and develop the technique. These lime-alumina samples were synthetically prepared from chemically pure $CaCO_3$

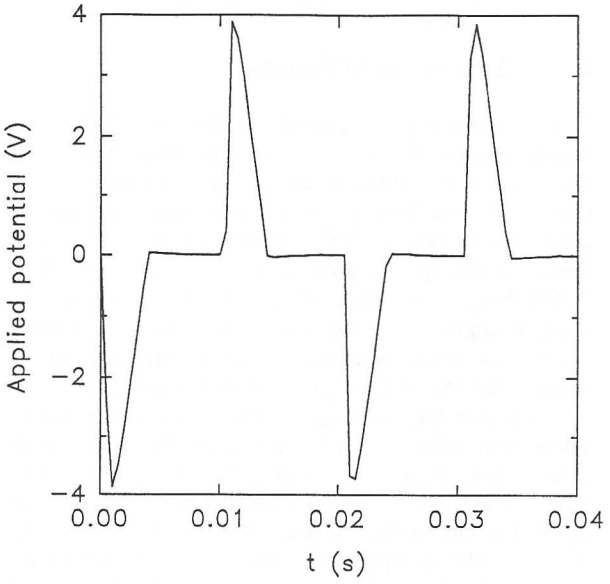

Fig. 2. Typical potential applied across the thermocouple during heating.

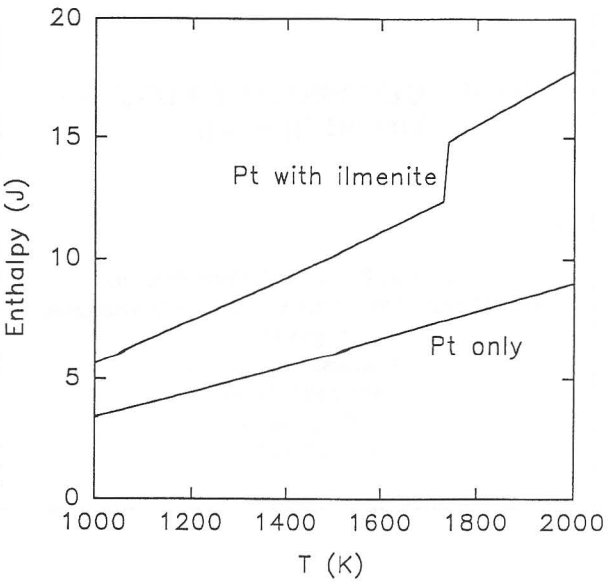

Fig. 3. The calculated temperature dependence of the enthalpy of a thermocouple with and without a slag sample. The curve marked "Pt only" is for the thermocouple itself (with a mass of 34 mg [7.5×10^{-5} lb]), while the curve labelled "Pt with ilmenite" is for a thermocouple of the same mass, containg 4 mg (9×10^{-6} lb) of ilmenite.

and Al_2O_3. The samples were pelletised, sintered in air (at 1200 to 1400 °C [2190 to 2550 °F] for 8 hours) and ground, repeating the process three times to obtain a homogeneous sample. The homogeneity of the sample was tested by conducting several liquidus determinations on different samples taken from the main sample. Homogeneity was assumed when these determinations indicated similar results.

The FeO-TiO_2 samples were prepared from chemically pure Fe, Fe_2O_3 and TiO_2, using the equation

$$Fe + Fe_2O_3 + 3TiO_2 \rightarrow 3FeO.TiO_2 \qquad (1)$$

to determine the stoichiometric amounts required to form ilmenite ($FeTiO_3$). Compositions above ilmenite were obtained by adding more TiO_2. Similar to the lime-alumina samples, these samples were pelletised, then sintered in dried, deoxidised argon (at 1250 °C [2280 °F] for 8 hours), quenched in water and ground, repeating the process five to seven times.

The samples were placed in the thermocouple as ground powders, using water as a temporary binding agent. The maximum particle size in the powders was determined by microscopic inspection to be 50 μm (0.0020").

2.3 Analysis of cooling curves

Thermal analysis based on cooling curves relies on the liberation of heat of solidification to alter the cooling rate, thus allowing the occurrence of solidification to be detected. However, solidification will only be detectable if the associated heat is large enough. In the configuration described here, the mass of the slag sample is much smaller than that of the thermocouple, which limits the sensitivity. However, enthalpy calculations do indicate that solidification should be detectable: figure 3 gives the calculated temperature dependence of the enthalpy of a thermocouple wire with a length of 10 mm (0.394") and diameter of 0.45 mm (0.018") (giving a mass of 34 mg [7.5×10^{-5} lb], being the mass of that part of the thermocouple which contains the slag sample), with and without a slag sample weighing 4 mg (9×10^{-6} lb). In these calculations, the tabulated enthalpy[6] of pure platinum was used for the thermocouple, and that of ilmenite for the slag. It is apparent that the heat of solidification forms a significant part of the enthalpy change upon cooling.

A second principle underlying the use of thermal analysis is the assumption that the fraction of liquid in the slag changes rapidly at the liquidus and solidus temperatures, allowing the observation of changes in cooling rate at well-defined temperatures. Calculation of the equilibrium fraction of liquid does indicate that the amount of liquid changes rapidly at both the solidus and liquidus temperatures, as shown in figure 4b. The calculations are based on the assumed eutectic phase diagram with no solid solubility range as shown in figure 4a. Inspection of published phase diagrams for ceramic systems shows this to be typical. It can be shown that the equilibrium fraction of liquid depends in the following way on temperature:

$$f_l = \frac{f_E}{1 - \phi(1 - f_E)} \qquad (2)$$

where f_l is the fraction of liquid, f_E is the fraction of eutectic component in the solidified slag, and ϕ is the dimensionless temperature, defined as follows:

$$\phi = \frac{T - T_E}{T_{liq} - T_E} \qquad (3)$$

where T is the actual temperature, and (as indicated in figure 4a) T_{liq} is the liquidus temperature for the specific composition, and T_E is the eutectic temperature.

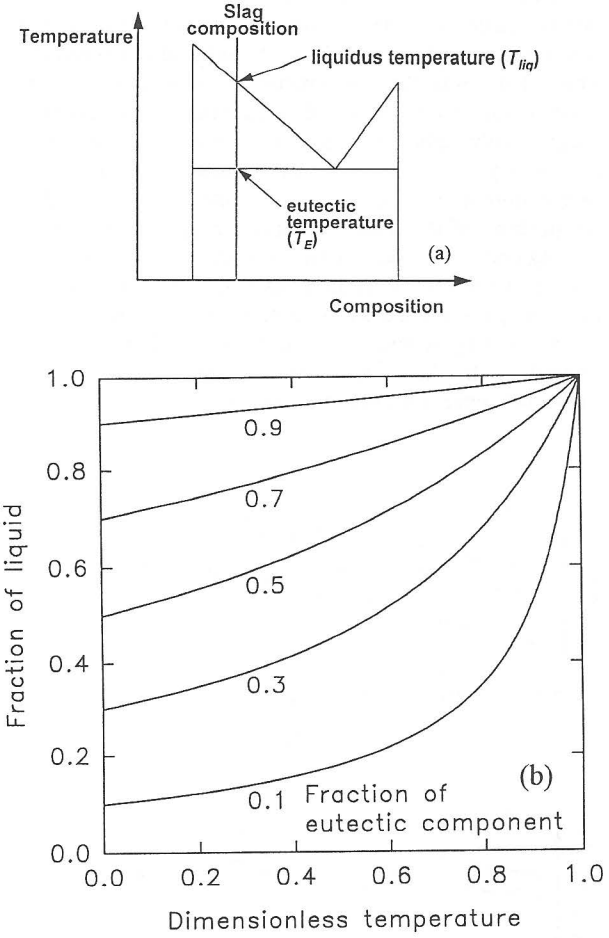

Fig. 4. Calculated temperature dependence of the fraction of liquid in an off-eutectic slag sample.
(a) Assumed eutectic phase diagram.
(b) Calculated amount of liquid, as a function of the dimensionless temperature coefficient (as defined in equation 3).

The calculated equilibrium fraction of liquid (figure 4b) shows that, in addition to the discontinuous change in the amount of liquid at the eutectic temperature, the fraction of liquid changes most rapidly at the liquidus temperature, indicating that both proeutectic and eutectic solidification should be clearly defined on the cooling curves. This was indeed found experimentally, as illustrated by figures 5a and 5b. This pair of figures shows the cooling curve (figure 5a) and the cooling rate as a function of temperature (figure 5b). As with all the cooling curves used in this work, this was measured by sampling the thermal EMF at a rate of 2 kHz for eight seconds after terminating the power supply to the thermocouple.
Figure 5 indicates that well-defined changes ("peaks") in the cooling rate – apparently due to proeutectic and eutectic solidification respectively – can be measured during cooling. However, the actual liquidus and solidus temperatures of this specimen are indicated on figure 5b,

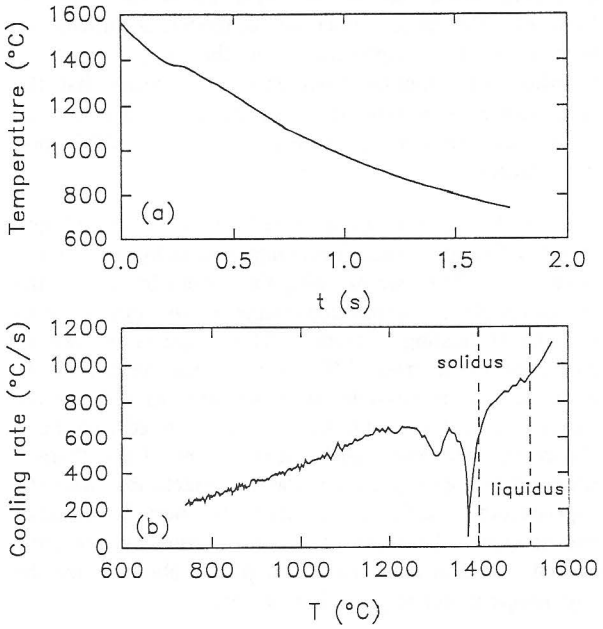

Fig. 5. Thermal analysis of a slag sample with a composition of 30%FeO-70%TiO_2.
(a) Cooling curve.
(b) Changes in the cooling rate along the cooling curve. Clear peaks are observed, but these are displaced to temperatures lower than the actual liquidus and solidus temperatures which are indicated on the graph.

showing the peaks to be displaced to lower temperatures. This indicates that the temperature at which the peaks are observed cannot be used as a reliable indication of the liquidus and solidus temperatures. At least two causes are thought to be responsible for this deviation: firstly, undercooling is required for nucleation of the solid phase(s), and, secondly, a temperature gradient arises along the length of the thermocouple tip during cooling. The second effect is a significant one, which can be evaluated as follows: it can be shown that, if a body is subjected to cooling at a constant rate, with one-dimensional heat conduction from one end, and with the other end thermally insulated, the temperature difference along the length of the body is given by:

$$\Delta T = \frac{dT}{dt}\frac{x^2}{2\alpha} \qquad (4)$$

where ΔT is the temperature difference, dT/dt is the cooling rate, x is the length of the body, and α is the thermal diffusivity of the material. Taking the properties of platinum at room temperature[7], its thermal diffusivity is

calculated to be 2.5×10^{-5} m^2/s (2.7×10^{-4} ft^2/s). Since a plane of symmetry (such as that through the tip of the thermocouple) behaves as a plane of thermal insulation, the appropriate length x is half the length of the wire around the slag sample, which gives x=5 mm (0.197"). Figure 5 shows the initial cooling rate to be as high as 500 °C/s (900 °F/s). This means that the calculated temperature difference along the thermocouple tip is some 250 °C (450 °F). This large temperature difference is sufficient to give substantial displacement of the peaks, which – together with possible undercooling – means that the temperatures at which the peaks are observed cannot be taken as reliable measures of the solidification temperatures.

It should be possible to reduce the effects of both undercooling and nonuniform temperatures by cooling at a lower rate. One way of doing this would be to cool the thermocouple in a controlled manner by the application of a reduced heating current. This requires a way of measuring the thermal EMF while applying the current. In principle, this is possible since the thyristor reduces the current to zero at some stages of the altered sine wave (figure 2). However, such measurement of the thermal EMF while applying power was not practicable with the experimental configuration since the periods of zero applied current (as supplied by the thyristor) were severely limited – and in some cases completely absent – for the high temperatures required in this work.

Instead, the effects of undercooling and nonuniform temperatures during cooling were avoided by analysing the cooling curve not for the *position* of the peaks, but for their presence. The underlying ideas are that the *presence* of the peak on the cooling curve is taken as an indication that liquid was present at the temperature from which cooling started, and that the *size* of the peak gives a rough indication of the amount of liquid that was present. Based on these ideas, the following procedures were formulated to determine the solidus and liquidus temperatures:

Liquidus temperature:

The thermocouple with the sample was initially heated to a temperature (which would be just above the solidus, although this would be unknown at this stage) where the liquid component of the sample is sufficient to allow the slag to flow between the two thermocouple wires, thus ensuring thermal contact between the thermocouple wire and sample. A concave meniscus between the two wires was taken to be indicative of this. Following this, the sample was consecutively heated to progressively higher starting temperatures (the starting temperature being the temperature at which the power supply was terminated), each time measuring a cooling curve, until the higher-temperature peak on the cooling curve (taken to represent pro-eutectic solidification), did not become larger with higher starting temperatures. The liquidus temperature was recorded as the average between the highest two starting temperatures where a difference in peak size was present. Figure 6a gives an example of such cooling curves.

Solidus temperature:

Similar to the liquidus temperature determinations the sample had to be heated initially to ensure thermal contact between the slag and wire. However, it was important to heat the sample intended for solidus temperature determinations above the liquidus followed by slow cooling at approximately 1 °C (1.8 °F) per second before attempting to determine the solidus. (This procedure proved necessary after a sample of 30%FeO-70%TiO_2 appeared to form a metastable phase during rapid cooling – with a solidus temperature considerably higher than that of the original composition.) The solidus was then determined as follows: after slow cooling from above the liquidus, the sample was heated to progressively higher starting temperatures, again recording the cooling curve from each temperature. The first starting temperature in this sequence was selected to correspond to the position of the lower solidification peak on the initial cooling curve. The solidus temperature was recorded as an average between the highest starting temperature which gave no peak on the subsequent cooling curve, and the lowest starting temperature which did yield such a peak (indicating that liquid had been present). An example of such a sequence is presented in figure 6b.

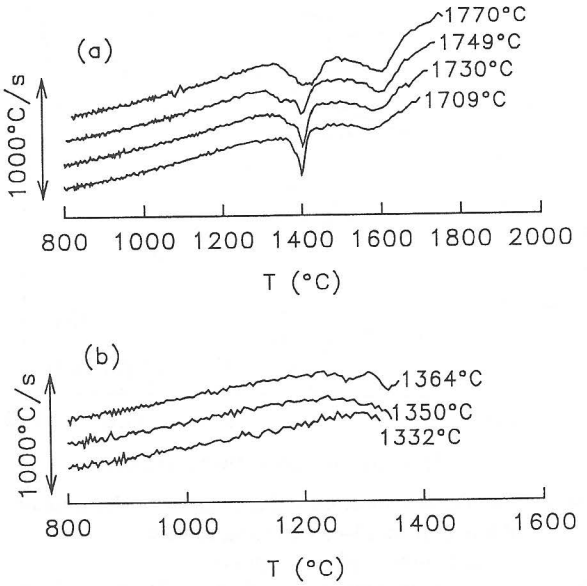

Fig. 6. Examples of cooling curves used to determine liquidus and solidus temperatures.

(a) Cooling curves for liquidus determination; slag sample with a composition of 72%CaO-28%Al_2O_3. The sample was cooled from progressively higher starting temperatures which are indicated to the right of each cooling curve. The liquidus temperature was measured as 1739 °C (3162 °F).

(b) Cooling curves for solidus determination; slag sample with a composition of 49%FeO-51%TiO_2. The sample was cooled from progressively higher starting temperatures which are indicated to the right of each cooling curve. The solidus temperature was measured as 1357 °C (2475°F).

Peak temperature determination:

As outlined above, determination of the liquidus and the solidus temperatures during heating involved cooling the sample from successively higher *known* temperatures. Although the temperature from which cooling had started could be determined accurately by analysing the cooling curve *after the fact*, practical execution of the measurements also required the temperature to be known while applying the heating power *before the start of cooling*. However, as mentioned above, it was not possible to measure the thermal EMF while the heating current was applied. To avoid this dilemma, the relationship between the heating power and the temperature was determined, and used to select approximate starting temperatures. The relationship is given in figure 7a, which gives the thermocouple temperature as a function of the root-mean-square (RMS) voltage across the thermocouple (since the thermal conductivity of platinum changes by only some 20% from room temperature to 1600K[8], the electrical resistance should change by a similarly small amount, and hence the heating power is approximately proportional to the square of the RMS voltage). Figure 7a shows the temperature to increase approximately linearly with the RMS voltage – hence the required power increases with the square of the peak temperature. This is the result of the combined effects of heat losses from the thermocouple by conduction (along the thermocouple wire), and radiation to the surroundings. A quantification of these heat losses is presented in Figure 7b. The heat losses were calculated by assuming the temperature profile to vary parabolically along the length of the thermocouple wire, according to the relationship

$$T = T_{tip} - \left(\frac{x}{l}\right)^2 \left(T_{tip} - T_o\right) \qquad (5)$$

where T is the temperature at a distance x from the tip of the thermocouple, T_{tip} is the temperature at the tip, and T_o is the temperature at a distance l from the tip. Such a parabolic temperature profile is obtained with uniform internal heat generation as with resistance heating[9]. The heat loss by conduction was calculated by applying Fourier's law of heat conduction at the position $x=l$, with l=10 mm and a thermal conductivity[7] of 71.6 $Wm^{-1}K^{-1}$. The approximate heat loss by radiation was obtained by integrating the Stefan-Boltzmann law along the length of the wire, as follows:

$$q_{rad} = 2\pi r\sigma\varepsilon \int_0^l \left(T^4 - T_\infty^4\right) dx \qquad (6)$$

where q_{rad} is the heat loss by radiation, r is the radius of the wire, ε is the emissivity of the wire(taken to be 0.15)[9], σ is the Stefan-Boltzmann constant, T is the local surface temperature, and T_∞ is the temperature of the surroundings (taken to be 298 K). The calculated heat losses in figure 7b indicate that the combination of the linear dependence of conductive heat loss on temperature, and the T^4 dependence of the radiative heat loss gives an approximate T^2 dependence of the total heat loss, in line with the measurements in figure 7a.

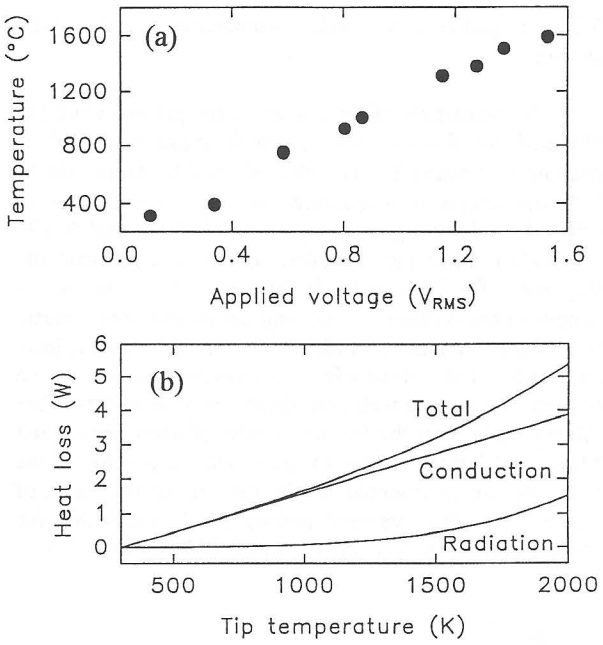

Fig. 7. Measured and calculated power requirements for heating the thermocouple

(a) Experimentally measured thermocouple temperatures, as a function of the alternating voltage applied across the thermocouple.

(b) Calculated heat loss for half the thermocouple. The three curves reflect the heat losses by radiation to the surroundings, conduction along the thermocouple wire and the total heat loss.

3. RESULTS AND DISCUSSION

3.1 Liquidus and solidus temperatures: CaO-Al_2O_3 system

Liquidus and solidus temperatures for two compositions in the CaO-Al_2O_3 system – measured with the procedure as outlined above – are compared in table I with the published data. It is clear that the correspondence is good, and that the technique may be used with some confidence.

Table I Comparison of the published liquidus and solidus temperatures for two CaO-Al_2O_3 compositions[10] with those measured with thermal analyses.

Composition (wt%)	39.6CaO-60.4Al_2O_3	28.3CaO-72.1Al_2O_3
% Eutectic component	42.4	61.1
Solidus (literature)	1395°C (2543°F)	1590°C (2894°F)
Solidus (measured)	not detected	1584°C (2883°F)
Liquidus (literature)	1564°C (2847°F)	1723°C (3133°F)
Liquidus (measured)	1566°C (2851°F)	1739°C (3162°F)

3.2 Liquidus and solidus temperatures: $FeO-TiO_2$ system

A comparison of the results of the present work (as obtained by thermal analysis) with those of Grau[1] is presented in figure 8. The method used by Grau was to heat the sample in a graphite resistance type furnace in dried, deoxidised argon to approximately 50 to 100 °C (90 to 180 °F) above the estimated liquidus and maintain the slag there for 15 minutes before terminating the power supply to the furnace. A cooling curve was continuously recorded (on a chart recorder) from the EMF output from an immersed thermocouple. The results obtained in the present work agree well with those reported by Grau, but differ greatly from the (earlier) results of MacChesney and Muan[2]. Melting points of pure TiO_2 reported in the literature are represented by the bar on the right axis of figure 8[3,10]; the measured melting point falls within the reported range 1825 °C (3317 °F) to 1857 °C (3375 °F).

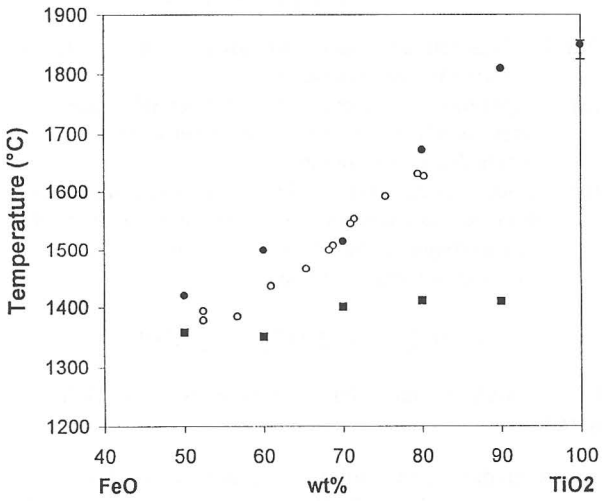

Fig. 8. A comparison of the liquidus and solidus temperatures obtained by thermal analysis (present work; filled circles) with those reported by Grau[1] (open circles). The bar at 100%TiO_2 represents the range of melting points of pure TiO_2 reported in the literature[3,10].

The absence of solidus points for slags containing more than 90%TiO_2 indicates that the solidus temperature could not be determined with certainty. This is presumably because these specimens contained a relatively small amount of eutectic component. It appears that the solidus temperature of specimens with less than some 50% eutectic component cannot be determined with the current thermal analysis procedure; this was also found for the $CaO-Al_2O_3$ system (Table I). This is certainly a limitation of the technique, although in the smelting process the liquidus temperature of the slag is probably of greater importance, especially for slags which contain relatively small amounts of a low-melting (eutectic) component.

4. CONCLUSION

(1) The main advantage of the thermal analysis technique is that it provides a rapid and accurate method for melting point determinations at temperatures of up to 1850°C (3360°F). One apparent limitation of the technique is that compositions with less than approximately fifty percent liquid at the eutectic temperature are not amenable to solidus temperature determinations.

(2) The procedure followed for liquidus temperature determinations was initial heating to above the solidus to ensure thermal contact between the sample and thermocouple wire, followed by heating to progressively higher starting temperatures, until the peak on the cooling curve which represents pro-eutectic solidification did not increase in size with increasingly higher starting temperatures. The liquidus temperature was recorded as the average between the two highest starting temperatures which did show an difference in peak size.

(3) The procedure followed to determine solidus temperatures was initial heating of the sample to above the liquidus temperature, followed by slow cooling to below 1000 °C (1832 °F). The sample was subsequently heated to progressively higher starting temperatures, starting at the temperature where the peak representing solidus solidification appeared upon cooling from above the liquidus temperature, and ending at the lowest starting temperature which yielded a solidification peak on the cooling curve. The solidus temperature was recorded as the average between the highest starting temperature where no peak appeared on the cooling curve and the lowest starting temperature where a peak did appear.

5. ACKNOWLEDGEMENT

The authors are grateful to ISCOR for their financial contribution to this work. We would also like to thank Gerrit van Rooyen, Andrie Garbers-Craig and Rian Dippenaar for their valuable suggestions and advice.

6. REFERENCES

1. A.E. Grau, "Liquidus Temperatures in the TiO_2-Rich Side of the $FeO-TiO_2$ System," Canadian Metallurgical Quarterly, Vol. 18, 1979, pp. 313-321.

2. J. B. MacChesney and A. Muan, "Phase equilibria at Temperatures in the system Iron Oxide - Titanium Oxide at Low Oxygen Pressures," The American Mineralogist, Vol.46, May - June 1964, pp. 572-582.

3. G. Eriksson and A.D. Pelton, "Critical Evaluation and Optimization of the Thermodynamic Properties and Phase Diagrams of the $MnO-TiO_2$, $MgO-TiO_2$, $FeO-TiO_2$, $Ti_2O_3-TiO_2$, Na_2O-TiO_2, and K_2O-TiO_2 Systems,"Metallurgical Transactions, Vol. 24B, October 1993, pp. 795-805.

4. P. R. Jochens, "Contribution to the Knowledge of the equilibrium and non-equilibrium Behaviour of Titaniferous Slags,", Ph.D. thesis, University of the Witwatersrand, 1968.

5. B. G. Baldwin, "The Liquidus and High-temperature Properties of Blast-furnace Slags," Journal of the Iron and Steel Institute, August 1957, pp. 388-395.

6. O. Kubaschewski, C.B. Alcock and P.J. Spencer, Materials Thermochemistry, 6th edition, Pergamon, Oxford, 1993, pp. 279, 304.

7. J. Elmsley, The Elements, Clarendon Press, Oxford, United Kingdom, 1989, pp. 140-141.

8. R.C. Weast (editor), CRC Handbook of Chemistry and Physics, 62nd edition, CRC Press, Boca Raton, Florida, 1981, p. E-9.

9. J.P. Holman, Heat Transfer, SI metric edition, McGraw-Hill, Singapore, 1989, pp. 38-39, 648.

10. Verein Deutscher Eisenhüttenleute, Slag Atlas, Verlag Stahleisen m.b.H, Düsseldorf, Germany, 1981, pp. 28, 31, 40, 49.

For further informantion on this paper, please contact Chris Pistorius at the Department of Materials Science and Metallurgical Engineering, University of Pretoria, Pretoria, 0002, SOUTH AFRICA, fax. no(+2712)3426812.